Filamentation-induced third-harmonic generation in air via plasma-enhanced third-order susceptibility

S. Suntsov,[1,*] D. Abdollahpour,[1] D. G. Papazoglou,[1,2] and S. Tzortzakis[1,†]

[1]*Institute of Electronic Structure and Laser, Foundation for Research and Technology Hellas, 71110, Heraklion, Greece*

[2]*Materials Science and Technology Department, University of Crete, 71003, Heraklion, Greece*

(Received 13 August 2009; published 10 March 2010)

We study, both experimentally and theoretically, the underlying physics of third-harmonic generation in air by a filamented infrared femtosecond laser pulse propagating through a thin plasma channel. It is shown that the recently observed more than two-order-of-magnitude increase of the efficiency of third-harmonic generation occurs due to the plasma-enhanced third-order susceptibility. An estimate of the effective value of this susceptibility is given.

DOI: 10.1103/PhysRevA.81.033817 PACS number(s): 42.65.Ky, 42.65.Re, 52.38.Hb

I. INTRODUCTION

In the last decade, fast progress in the development of the sources of high-energy pulses of subpicosecond duration opened new ways for improving the efficiency of nonlinear frequency conversion. In particular, considerable interest was attracted to harmonic generation since it enables the extension of coherent ultrashort-pulse radiation to an important short-wavelength region. In this regard, third-harmonic generation (THG) through filamentation of infrared (IR) femtosecond laser pulses in a variety of atomic and molecular gases has become one of the promising techniques for producing energetic pulses in the UV wavelength range [1–8]. However, conversion efficiency of this process was shown to be limited by several factors with the major one being the accumulated upon propagation phase-mismatch between the harmonic and the fundamental waves [5,7].

In a recent publication [9], we have reported a two-order-of-magnitude enhancement of the third-harmonic (TH) emission generated by a filamented IR femtosecond pulse. The TH enhancement, accompanied by significant spatial reshaping, appeared after the filament intersected a plasma string produced by another advancing femtosecond pulse. Comparable TH enhancement has also been observed by Hartinger and Bartels in various atomic and molecular gases [10]. Although strong correlation of THG efficiency with plasma density saturation and with its decay rate indicated that plasma presence was responsible for the observed effects [9], the underlying physical mechanism was not clearly understood. We contemplated two completely different approaches that could in principle explain the observed enhancement of THG efficiency. The enhancement of the TH generation could emerge from a bulk effect, that is, an increase of the nonlinear coefficient correlated with the presence of plasma as suggested in Refs. [11,12], or through a neutral air-plasma interface effect similar to that observed by Tsang at air-dielectric interfaces [13].

In this work, we study the physical mechanism that drives the TH emission enhancement. Based on experimental results, we show that the bulk plasma-enhanced nonlinear susceptibility and not the air-plasma interface effect, is responsible for the observed TH enhancement. Furthermore, we propose a phenomenological model and derive a simple expression for the TH intensity that quantifies the dependence of the TH signal on the plasma density. Using this model, which also takes into account phase matching between the fundamental and the harmonic waves in the plasma volume, we discuss the limitations of the technique in producing energetic pulses at third-harmonic frequency in a low-density plasma.

II. EXPERIMENTAL RESULTS AND DISCUSSION

The experiments were conducted using a Ti:sapphire chirped-pulse amplification laser system supplying 35-fs, 800-nm IR pulses with energies up to 30 mJ at a 50-Hz repetition rate. The schematic of the experimental setup is shown in Fig. 1. First, the fundamental laser beam was split into two arms, Pump and Filament, using a beamsplitter. Laser pulses in the Filament arm with 0.5-mJ energy were focused using a 100-cm-focal-length lens L1 creating a light filament in air with a length of about 5 cm. The filament interacted with the plasma string generated by pulses in the Pump arm that were focused perpendicularly to the Filament beam with a combination of a spherical (L2, focal length 10 cm) and a plano-convex cylindrical (CL, focal length $\infty/10$ cm) lens. This astigmatic arrangement leads to the generation of two orthogonally oriented plasma channels in the sagittal and meridional foci. By changing the distance between L2 and CL we were able to vary the length of the horizontally oriented plasma string in the meridional focus, while its spatial overlap with the filament was achieved by moving the two lenses as a whole along the Pump beam path. The delay between the pulses in the Filament and Pump arms was adjusted with an optical delay line. After the filament, a fused silica prism P was used to angularly separate the TH and fundamental waves. Finally, the TH energy was measured using a calibrated photodetector (D) which was preceded by an interference filter at 266 nm.

In order to study the nature of the physical mechanism responsible for the harmonic emission enhancement, we first need to distinguish between the two different mechanisms that could, in principle, explain the observed effect, namely the bulk

*ssuntsov@iesl.forth.gr

†stzortz@iesl.forth.gr; http://unis.iesl.forth.gr

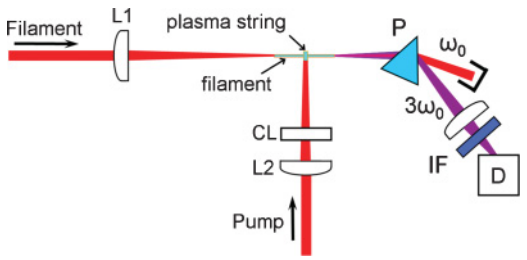

FIG. 1. (Color online) Experimental setup: L1, L2, lenses; CL, plano-convex cylindrical lens (cylindrical axis is parallel to the plane of the figure); P, prism; IF, interference filter at 266 nm; D, calibrated photodetector.

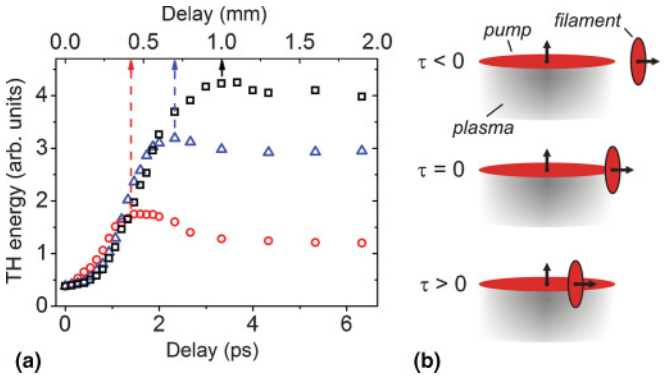

FIG. 2. (Color online) (a) TH energy as a function of the delay between the Pump and Filament pulses for Pump plasma channel thickness of 0.4 mm (circles), 0.7 mm (triangles), and 1 mm (squares). The locations of the harmonic signal maxima are indicated by vertical arrows. (b) Schematic of the relative position of the Pump and Filament pulses at different timing in the experimental geometry.

plasma properties and the neutral air-plasma interface. More specifically, the presence of charged species (free electrons and ions) can effectively increase the third-order nonlinear optical susceptibility of a medium [11,12]. Thus, the enhancement of TH generation in this case would be the result of a bulk effect in the plasma volume. On the other hand, since the refractive index of a medium changes in the presence of plasma, then by introducing the Pump plasma string we create an interface between the two media with different refractive indices (under our experimental conditions, this difference in air can be as high as 7×10^{-3} [14]). Therefore, at such an interface, the inversion symmetry of the bulk along the Filament beam propagation direction is broken, resulting in a field gradient that could be responsible for the enhancement of TH emission (see for example Ref. [13]).

In the case of bulk nature of the effect, one would expect the harmonic emission to grow with the plasma thickness (assuming all other parameters are the same), while this would have no effect in the case of the interface model, as the number of interfaces remains the same. So, in order to clarify the origin of the physical mechanism that drives the enhancement of the harmonic wave, we conducted TH generation experiments with various thicknesses of the Pump plasma string. Using the astigmatic two-lens arrangement, described above, we created three plasma strings in the Pump arm with different thicknesses of 0.4, 0.7, and 1 mm, respectively. To guarantee the same mean plasma density ($\sim 5 \times 10^{17}$ cm^{-3}) inside all three plasma strings, the Pump pulse energy was set at 2.5, 5, and 8 mJ, respectively. The total measured TH energy as a function of the delay τ between the Pump and Filament pulses for all three cases is shown in Fig. 2(a). For better understanding these results, a simple schematic of the relative position of the Pump and Filament pulses at different delays is shown in Fig. 2(b). We define a zero delay point as the delay at which the plasma, produced by the Pump pulse, starts to affect the Filament pulse propagation and, consequently, the energy of the harmonic emission. With further increase of the delay, the Filament pulse will interact with the remaining portion of the Pump plasma channel. Finally, the maximum interaction length will be achieved when the delay (expressed in millimeters of light propagation in air) becomes equal to the Pump plasma string thickness. Therefore, the delays that correspond to the maxima of the TH energy in Fig. 2(a) are equal to the respective plasma string thicknesses, namely 0.4, 0.7, and 1 mm. The results of Fig. 2(a) are a clear indication of the bulk nature of the effect since the maximum TH energy monotonically grows with the plasma thickness. Additionally, the concept of TH enhancement through an interface effect fails to predict our experimental results because in this case the TH energy should depend only on the number of interfaces, which in all three cases is constant (two interfaces). The observed subsequent drop in the harmonic emission in Fig. 2(a) at higher delays is due to the plasma density decay in the Pump channel, as was also observed in Ref. [9].

III. THEORETICAL MODEL

Since we have proven that the effect of interfaces in our case is not important during TH generation in a plasma channel, we focus on the concept of the enhanced bulk third-order optical susceptibility due to the presence of free-electron–ion plasma. Using this assumption and according to the well-known formula [15,16], the third-harmonic intensity for the case of a Gaussian beam focused in the middle of a plasma medium can be written as

$$I_{3\omega}(\Delta k, L) = \frac{(3\omega)^2}{n_{3\omega} n_\omega^3 c^4 \varepsilon_0^2} \left|\chi_{pl}^{(3)}\right|^2 I_\omega^3 \left| \int_{-L/2}^{L/2} \frac{\exp(i\Delta k z)}{(1 + iz/z_R)^2} dz \right|^2, \quad (1)$$

where $\chi_{pl}^{(3)}$ is the plasma-enhanced third-order susceptibility, I_ω is the fundamental intensity, $\Delta k = 3k_\omega - k_{3\omega}$ is the total wave-vector mismatch between the fundamental and TH waves, L is the plasma thickness, z_R is the Rayleigh length, and n_ω and $n_{3\omega}$ are the refractive indices at the fundamental and TH frequency, respectively. Equation (1) takes into account the generation of the third-harmonic wave in the bulk of an ionized medium due to effective third-order susceptibility, as well as the effect of the phase mismatch between the fundamental and harmonic waves due to chromatic dispersion. Although Eq. (1) is written for continuous-wave beams, it still holds for ultrashort pulses under our experimental conditions, since the maximum calculated walk-off between the fundamental and TH pulses caused by the group velocity dispersion in a thin plasma layer of ionized air does not exceed 1 fs. In a quasiplanar limit for the fundamental wave phase front

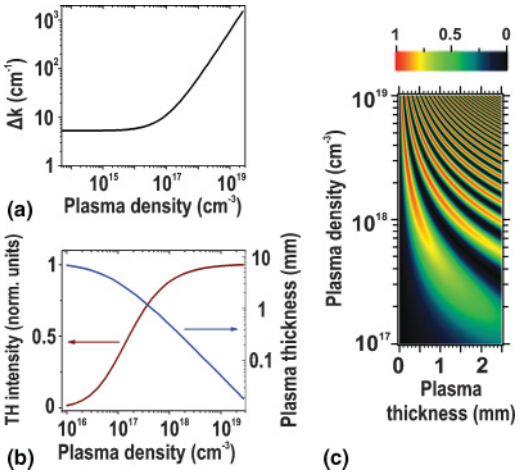

FIG. 3. (Color online) (a) Total wave-vector mismatch Δk between 800 and 267 nm wavelengths as a function of plasma density. (b) Maximum TH intensity in normalized units (left vertical scale) and minimum plasma thickness L needed to reach it (right vertical scale) versus electron density. (c) False color two-dimensional map of TH intensity versus plasma density and plasma thickness (normalized units).

($L \ll z_R$), which was also the case in our experiments, Eq. (1) can be simplified to

$$I_{3\omega}(\rho_e, L) \propto \left|\chi_0^{pl(3)}\right|^2 \rho_e^2 \frac{\sin^2(\Delta k L/2)}{(\Delta k/2)^2}, \tag{2}$$

where we replaced $\chi_{pl}^{(3)}$ with $(\chi_0^{pl(3)}\rho_e)$ where $\chi_0^{pl(3)}$ is the specific effective third-order optical susceptibility, and ρ_e is the plasma density (representing the density of the effective nonlinear medium).

It is worth noticing that the wave-vector mismatch Δk in Eq. (2) is itself a function of the plasma density. The absolute value of the total wave-vector mismatch as a function of the plasma density, calculated using the Sellmeier equation for atmospheric density air [17] and the Drude model for plasma [14], is plotted in Fig. 3(a). Clearly, since there is always nonzero Δk, on-axis third-harmonic generation in plasma is not phase matched. Let us now analyze how the harmonic intensity given by Eq. (2) depends on the plasma density ρ_e. As can be seen in Fig. 3(a), for densities up to 10^{16} cm^{-3} the wave-vector mismatch is nearly constant ($\sim$5.3 cm^{-1}) because the major contribution to it comes from the linear dispersion of air. Therefore, in the low plasma density limit, Eq. (2) can be written as $I_{3\omega} \propto \rho_e^2$, $\rho_e \leqslant 10^{16}$ cm^{-3}. On the other hand, at densities in excess of 5×10^{17} cm^{-3} Δk is dominated by the plasma-induced refractive index changes and is linearly proportional to the plasma density. Hence, in the high plasma density limit, Eq. (2) becomes: $I_{3\omega} \propto \sin^2(\text{const} \times \rho_e L)$, $\rho_e > 5 \times 10^{17}$ cm^{-3}. This formula predicts oscillations of the harmonic intensity as the plasma density ρ_e or plasma thickness L are increased while the oscillation amplitude is no longer dependent on ρ_e. Figure 3(c) shows the two-dimensional map of TH intensity versus plasma density and its thickness, calculated using Eq. (2). Also, the maximum harmonic intensity and the minimum plasma thickness needed to reach it are plotted in Fig. 3(b) as a function of plasma density. Clearly, to generate stronger harmonic signal, it is advantageous to use higher density (and, respectively, thinner) plasma string. In any case, the TH signal will finally saturate as a consequence of the already discussed independence of the amplitude of the TH intensity oscillations on ρ_e at high plasma densities. This limits the efficiency of the TH generation achievable with the described technique. To further increase the efficiency, other techniques should be used (e.g., quasi-phase-matched plasma structure such as an optically preformed periodic plasma waveguide [18] or plasma with density ripple [19]).

To verify the proposed phenomenological approach, we measured first the TH signal as a function of Pump pulse energy. As in our previous work [9], a thin ($<$100 μm) plasma string was produced in the Pump arm using a single 10-cm-focal-length spherical lens. Since the theoretical harmonic intensity of Eq. (2) is given in terms of plasma density, the next important step was to find the correlation of plasma density and the thickness of the produced plasma channel with the Pump pulse energy. This was done using independently in-line holographic and electric conductivity techniques whose detailed description can be found in Refs. [14] and [20], respectively. Our measurements showed that as the pump pulse energy varied from 0.15 to 1.5 mJ, the peak plasma density ρ_e and the effective thickness L varied in a range 7×10^{18} cm^{-3} to 1.55×10^{19} cm^{-3}, and 8 to 38 μm, respectively. In Fig. 4 we compare the normalized theoretical and experimentally measured TH intensities plotted as a function of plasma density. The theoretical points were calculated by substituting the experimentally measured values of the plasma string density and thickness into Eq. (2). The agreement between the theoretical predictions and the experimental values is excellent.

Despite the significant number of theoretical studies in the literature on third-harmonic generation in plasmas, most of them consider dense fully ionized plasmas and/or relativistic regime (laser intensities above 10^{18} W/cm^2). A consistent quantum-mechanical analysis of THG in low-density gaseous plasma under conditions close to those in our experiments is missing. However, the successful prediction of the behavior of the TH intensity by the simple phenomenological model of the enhanced third-order susceptibility enables us to go one step further and give a rough estimate of the $\chi_{pl}^{(3)}$ value.

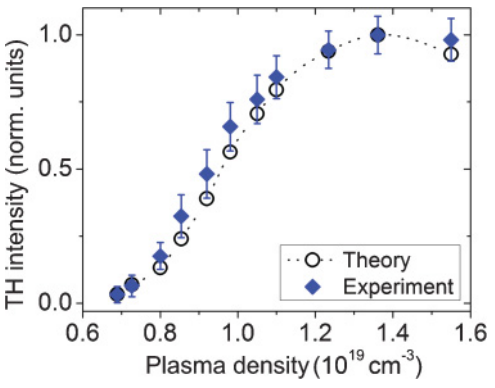

FIG. 4. (Color online) Theoretical (circles) and experimentally measured (diamonds) normalized TH intensity as a function of the plasma density in the Pump channel.

This can be done using Eq. (1) and the results of our previous work [9], where approximately 250 times enhancement of TH intensity was achieved upon intersecting the filament by a thin ($L \sim 30$ μm), dense ($\rho_e \sim 2 \times 10^{19}$ cm^{-3}) plasma channel. We estimate that during the filamented pulse propagation in air under our experimental conditions, the peak fundamental intensity I_ω reached $(5 \pm 2) \times 10^{13}$ W/cm^2 [21]. The value of the peak harmonic intensity $I_{3\omega} \sim (1.2 \pm 0.6) \times 10^{12}$ W/cm^2 was found using the measured TH pulse energy 0.6 μJ, the estimated harmonic pulse duration of (30 ± 3) fs, and the TH beam near-field diameter of (50 ± 10) μm [9]. By substituting these numbers into Eq. (1), we estimate $\chi^{(3)}_{pl}$ to be approximately equal to $(4.5 \pm 3) \times 10^{-24}$ m^2/V^2. This number is more than one order of magnitude higher than the third-order nonlinear susceptibility of air $\chi^{(3)}_{\text{air}} \sim 1.1 \times 10^{-25}$ m^2/V^2 (corresponds to the Kerr nonlinear coefficient of atmospheric pressure air $n_2 \sim 3.2 \times 10^{-19}$ cm^2/W [22]).

IV. CONCLUSION

In summary, we have shown that enhancement of third-harmonic wave generated within femtosecond IR filament in air when it crosses a thin plasma string, created by another advancing focused laser pulse, is a bulk process that does not rely on the properties of the produced neutral air-plasma interfaces. Despite the complex dynamics arising from a variety of linear and nonlinear effects involved, the more than two-order-of-magnitude increase of third-harmonic generation efficiency in a presence of the relatively low density ($\rho_e < 2 \times 10^{19}$ cm^{-3}) plasma string can be satisfactorily described by an effective, plasma-enhanced third-order optical susceptibility. Using this simple phenomenological approach, we are able to accurately describe the functional dependence of the THG enhancement on the plasma density. Our results suggest using free-electron–ion plasma as a nonlinear medium for efficient wave-mixing processes such as generation of energetic XUV pulses, or could eventually explain the strong THz emission from filaments in air [21].

ACKNOWLEDGMENTS

This work was supported by the European Union Marie Curie Excellence Grant "MULTIRAD" under Grant No. MEXT-CT-2006-042683.

[1] S. Backus, J. Peatross, Z. Zeek, A. Rundquist, G. Taft, M. M. Murnane, and H. C. Kapteyn, Opt. Lett. **21**, 665 (1996).
[2] C. W. Siders, N. C. Turner III, M. C. Downer, A. Babine, A. Stepanov, and A. M. Sergeev, J. Opt. Soc. Am. B **13**, 330 (1996).
[3] A. B. Fedotov, N. I. Koroteev, M. M. T. Loy, X. Xiao, and A. M. Zheltikov, Opt. Commun. **133**, 587 (1997).
[4] J. Peatross, S. Backus, J. Zhou, M. M. Murnane, and H. C. Kapteyn, J. Opt. Soc. Am. B **15**, 186 (1998).
[5] H. R. Lange, A. Chiron, J.-F. Ripoche, A. Mysyrowicz, P. Breger, and P. Agostini, Phys. Rev. Lett. **81**, 1611 (1998).
[6] N. Aközbek, A. Iwasaki, A. Becker, M. Scalora, S. L. Chin, and C. M. Bowden, Phys. Rev. Lett. **89**, 143901 (2002).
[7] N. Kortsalioudakis, M. Tatarakis, N. Vakakis, S. D. Moustaizis, M. Franco, B. Prade, A. Mysyrowicz, N. A. Papadogiannis, A. Couairon, and S. Tzortzakis, Appl. Phys. B **80**, 211 (2005).
[8] M. Kolesik, E. M. Wright, A. Becker, and J. V. Moloney, Appl. Phys. B **85**, 531 (2006).
[9] S. Suntsov, D. Abdollahpour, D. G. Papazoglou, and S. Tzortzakis, Opt. Express **17**, 3190 (2009).
[10] K. Hartinger and R. A. Bartels, Appl. Phys. Lett. **93**, 151102 (2008).
[11] A. B. Fedotov, S. M. Gladkov, N. I. Koroteev, and A. M. Zheltikov, J. Opt. Soc. Am. B **8**, 363 (1991).
[12] R. A. Ganeev, M. Suzuki, M. Baba, H. Kuroda, and I. A. Kulagin, Appl. Opt. **45**, 748 (2006).
[13] T. Y. F. Tsang, Phys. Rev. A **52**, 4116 (1995).
[14] D. G. Papazoglou and S. Tzortzakis, Appl. Phys. Lett. **93**, 041120 (2008).
[15] J. F. Ward and G. H. C. New, Phys. Rev. **185**, 57 (1969).
[16] R. W. Boyd, *Nonlinear Optics* (Academic Press (UK), London, 1992).
[17] K. P. Birch and M. J. Downs, Metrologia **31**, 315 (1994).
[18] C.-C. Kuo, C.-H. Pai, M.-W. Lin, K.-H. Lee, J.-Y. Lin, J. Wang, and S.-Y. Chen, Phys. Rev. Lett. **98**, 033901 (2007).
[19] D. Dahiya, V. Sajal, and A. K. Sharma, Phys. Plasmas **14**, 123104 (2007).
[20] S. Tzortzakis, M. A. Franco, Y.-B. André, A. Chiron, B. Lamouroux, B. S. Prade, and A. Mysyrowicz, Phys. Rev. E **60**, R3505 (1999).
[21] A. Couairon and A. Mysyrowicz, Phys. Rep. **441**, 47 (2007).
[22] A. Couairon, S. Tzortzakis, L. Bergé, M. Franco, B. Prade, and A. Mysyrowicz, J. Opt. Soc. Am. B **19**, 1117 (2002).